PHYSICAL REVIEW A **76**, 042714 (2007)

Probing final-state interactions in the photodetachment from OH^-

G. Aravind,[1] A. K. Gupta,[2] M. Krishnamurthy,[1] and E. Krishnakumar[1,*]
[1]*Tata Institute of Fundamental Research, Homi Bhaba Road, Mumbai 400 005, India*
[2]*Bhabha Atomic Research Centre, Mumbai 400 085, India*
(Received 18 July 2007; published 24 October 2007)

Angular distributions of photoelectrons in the photodetachment from $OH^-(^1\Sigma^+)+h\nu \rightarrow OH(^2\Pi_i;\upsilon=0)+e^-$ process were measured at four discrete wavelengths (440–266 nm) using a crossed anion-laser interaction and a linear time-of-flight photoelectron spectrometer. The asymmetry parameters determined from the measured angular distributions at these wavelengths were fitted to a model that accounts for the dipole interaction between the final-state particles and to a free-electron form of the Cooper-Zare model. The observed spectral dependence of the asymmetry parameter shows no significant influence of the dipole interaction. The spectral dependences of the asymmetry parameter in the photodetachment from OH^- and the previously studied O^- are found to be very similar.

DOI: 10.1103/PhysRevA.76.042714 PACS number(s): 33.80.Eh

I. INTRODUCTION

Negative ions play vital roles in processes that occur in a variety of environments like stellar and planetary atmospheres, laboratory and industrial plasmas [1,2], and various other fields. They are an ideal "laboratory" to study the structure and dynamics of systems with short-range interactions like that between the electron and the neutral core. The electron-electron correlation effects principally determine the structure and dynamics of anions, and thus experimental studies on anions help in critically evaluating the theoretical models that account for electron correlations [3]. Advancements in laser technology [4], the availability of versatile anion sources [5], storage rings [6], and advanced spectrometric techniques such as photoelectron imaging [7] have greatly motivated negative ion research in recent years. There are excellent reviews on various aspects of negative ion research [3,5,8–11].

Photodetachment from negative ions is a versatile technique that has often been employed in studies on the structure and dynamics of negative ions. The photodetachment technique is an excellent probe for relativistic and other weak effects, such as electron correlations, which are overshadowed by long-range Couloumb interactions in photoionization processes. Andersen *et al.* [8] discuss various specialized techniques employed in photodetachment studies.

Total photodetachment cross section and angular distribution measurements carry most of the information related to the dynamics of the photodetachment process. The asymmetry parameter for the photoelectron angular distribution contains all the details about the dynamics relevant to the angular distribution of photoelectrons [12]. The spectral dependence of the asymmetry parameter near autodetaching resonances can reveal the role of spin-orbit interactions in the photodetachment as well as photoionization processes [13]. The spectral dependence of the asymmetry parameter can be a probe for the nature of final-state interactions in the photodetachment process [14]. Though the angular distribution of photoelectrons was measured in the past for many anions, relatively few anions have been studied for the spectral dependence of their asymmetry parameters. Hanstorp *et al.* [15] studied the spectral dependence of angular distribution in the photodetachment from O^-. He^- [16], B^- [17], C^- [18], Al^-, Si^-, P^- [19], Ge^- [20], Sn^- [21], and V^- [22] are the few other anions for which the spectral dependence of the photoelectron angular distributions was studied in the past.

It is surprising to note that all of the experimental studies on the spectral dependence of the asymmetry parameter were done for photodetachment from atomic anions, while, to the best of our knowledge, there is no such study on a molecular anion. Mabbs *et al.* [23] study the spectral dependence of the asymmetry parameter in the photodetachment from iodide clusters. Their study shows the anomalous nature of the photodetachment from $CH_3I \cdot I^-$, revealing the role of the solvent in photodetachment. Such anomalous behavior in the photodetachment of clusters motivates the study of the spectral dependence of the asymmetry parameter for molecular anions. The interactions between the ejected electron and the neutral remnant are principally determined by the long-range forces between the final-state particles. These are the interactions that govern the behavior of the near-threshold photodetachment cross sections. The longest-range interaction in the photodetachment from an atomic anion is due to the $l(l+1)/r^2$ centrifugal potential experienced by the detached electron of angular momentum l. Apart from the centrifugal interaction, if the remnant molecule is a dipole, photodetachment may result in an r^{-2} form of dipole interaction between the neutral molecular dipole and the detached electron. In this case, the so-called Wigner threshold law [24] is no longer valid and the modified threshold laws given by O'Malley [25] need to be considered. It is important to explore the possibilities of unraveling information relevant to the molecular dynamics through angular distribution studies on molecular anions. Can we probe the effects of the remnant molecular environment, such as the dipole interactions, on the photodetached electron? Can we understand the delocalization of the attached "extra" electron in the molecular anions? We studied the photodetachment from OH^- as an attempt to address these questions. Though OH^- has been the subject of a number of photodetachment studies [26–32], to

---

[*] ekkumar@tifr.res.in

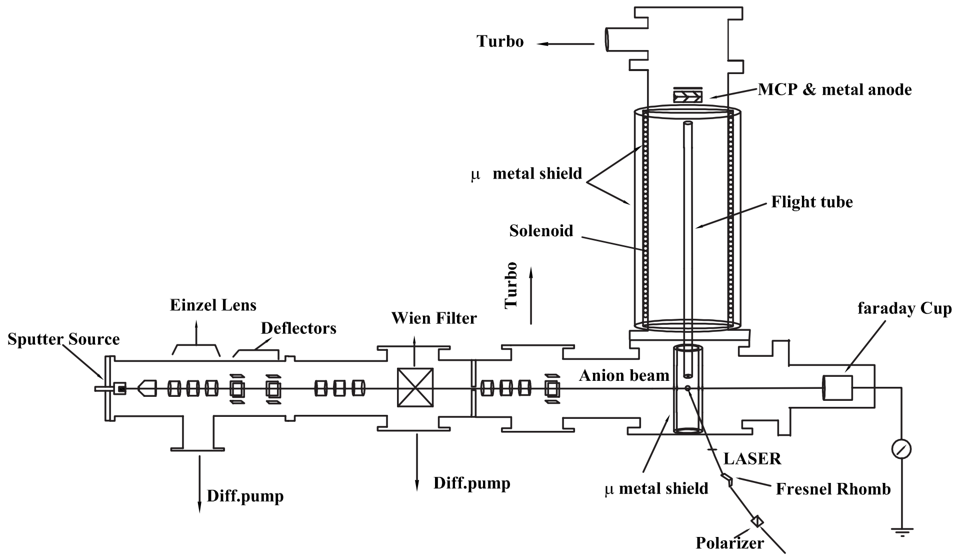

FIG. 1. Schematic diagram of the anion photodetachment experimental apparatus. The total ion beam path was about 1.5 m.

the best of our knowledge, this is the first report on the spectral dependence of the asymmetry parameter for OH^- or any molecular anion.

II. EXPERIMENTAL METHOD

Figure 1 shows the schematic diagram for the anion photodetachment experimental apparatus. A detailed discussion of the newly constructed photodetachment experimental arrangement is provided in a recent article [14] and we briefly describe the same here. Anions were produced using a Cs sputter source [33]. A mixture of iron oxide and titanium hydride was used as cathode pellet for producing OH^- anions. The sputtered negative ions are extracted and accelerated to about 3 kV. Anions are focused onto the Wien mass analyzer using two sets of Einzel lenses. The mass-analyzed anion current of about 100 nA is transported to the interaction region using another Einzel lens and deflector plates. The ion source region was maintained at 1×10^{-7} Torr using a diffusion pump. The interaction chamber was essentially a six-way cross made out of nonmagnetic stainless steel. The linear time-of-flight spectrometer of 1 m length is mounted with its axis perpendicular to both the anion and laser beam path. The interaction chamber is maintained at high vacuum of about 1×10^{-8} Torr using a turbomolecular pump backed by an oil-free pump. The detector region was maintained at 1×10^{-8} Torr using another turbomolecular pump. The region pumped by the diffusion oil pump was differentially isolated from the interactive region. This is essential to minimize the background electrons due to collisions with the background gas and the possible multiphoton ionization of large background molecules. The flight tube and the interaction region were shielded from Earth's magnetic field using two separated layers of μ-metal sheets. A pair of microchannel plates of 40 mm diameter, in chevron configuration, were used for electron detection.

The photon beams were produced using a neodymium-doped yttrium aluminum garnet (Nd:YAG) laser and an excimer-pumped dye laser. The dyes used for the measurements were Coumarin 2 (440 nm) and Stilbene 3 (400 nm). The laser polarization was rotated using a double Fresnel rhomb. The laser beam size at the interaction region was about 3 mm in diameter. The angular resolution for the measurements was ±6°.

The microchannel plate detector signal was amplified and then processed using a constant fraction discriminator (CFD). The voltage signal output of a photodiode triggered by the laser pulse was used as a "start" for the time-to-amplitude converter (TAC). The output pulse of the CFD was fed to the "stop" of the TAC. Detachment due to collisions with the background gas is a major problem in experiments with fast negative ion beams. This problem was effectively handled by maintaining high vacuum in the interaction region. Since the electrons were detected in a counting mode, we had to be careful about possible pileup. The count rate was only a few photoelectrons per second at a laser repetition rate of 100 Hz, thus making pileup negligible.

At the vacuum of 1×10^{-8} Torr, in the presence of only the ion beam, the background electron count rate was 100 per second. During the laser photodetachment measurements, the electron collection was only in a narrow time window of 1.5×10^{-6} s for each laser pulse. Thus for the laser repetition rate of 100 Hz we have 0.015 background electrons per second. Thus we could achieve a signal-to-noise ratio much better than 200 near the photoelectron peak. We also checked the background contributions of secondary electrons through multiphoton ionization by the laser without the anion beam and found it to be nil.

III. RESULTS AND DISCUSSION

Figure 2 shows the photoelectron spectrum for the $OH^-(^1\Sigma^+) + h\nu \rightarrow OH(^2\Pi_i; v=0) + e^-$ process at 355 nm. The resolution of our linear time-of-flight spectrometer is 50 meV at 1 eV.

The photoelectron angular distribution was obtained by recording the photoelectron spectra for every 8° rotation of a double Fresnel rhomb, i.e., in steps of 16°. The photoelectron

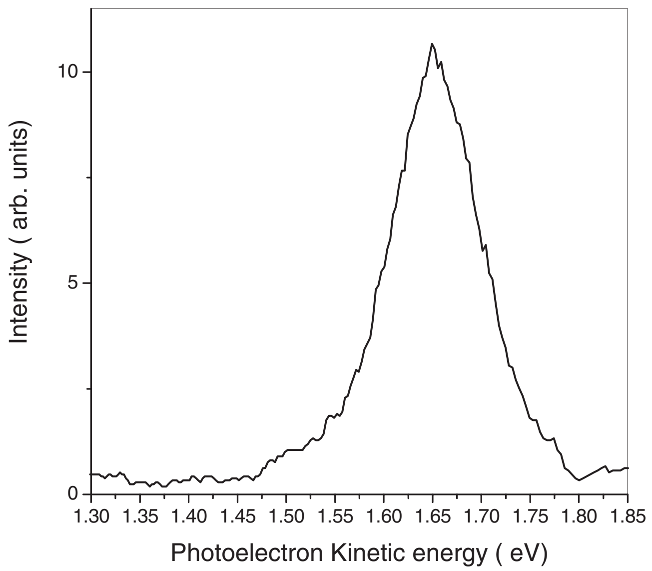

FIG. 2. Photoelectron spectrum for $\mathrm{OH}^-({}^1\Sigma^+)+h\nu\rightarrow\mathrm{OH}({}^2\Pi_i)+e^-$ transition at 355 nm.

yield was taken to be the area under the peak in the photoelectron spectra. The asymmetry parameter was then obtained by least-squares fitting the yield obtained for various linear polarization angles with respect to the electron collection direction to $Y(\theta)=a[1+\beta P_2(\cos(\alpha-\phi))]$, where $P_2[\cos(\theta)]$ is the second-order Legendre polynomial, α is the dial reading on the double Fresnel rhomb mount, and a, β, and ϕ are parameters in the least-squares fit. As mentioned earlier, the angular resolution of our spectrometer is about 6° and was taken into account during the least-squares fitting.

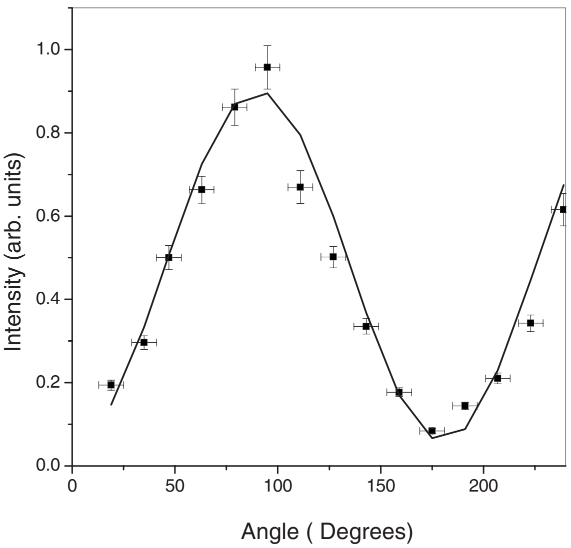

FIG. 3. Photoelectron angular distribution for $\mathrm{OH}^-({}^1\Sigma^+)+h\nu\rightarrow\mathrm{OH}({}^2\Pi_i)+e^-$ process at 440 nm. The normalized photoelectron yield was recorded while rotating the double Fresnel rhomb in steps of 8°. The measured normalized yield was then least-squares fitted to $Y(\theta)=a[1+\beta P_2(\cos(\alpha-\phi))]$ and the fit is shown as the solid line. The error bars for the normalized yield show one standard deviation and those for the angle represent 6° angular resolution in our measurements. The data were convoluted for a finite acceptance angle.

TABLE I. Measured asymmetry parameters for $\mathrm{OH}^-({}^1\Sigma^+)+h\nu\rightarrow\mathrm{OH}({}^2\Pi_i)+e^-$ photodetachment process at four different wavelengths.

Wavelength (nm)	Photoelectron energy (eV)	Asymmetry parameter β
440	0.98	-0.90 ± 0.04
400	1.26	-0.83 ± 0.02
355	1.65	-0.72 ± 0.03
266	2.81	-0.22 ± 0.03

The experimental arrangement and the measurement procedure were tested by performing angular measurements for $\mathrm{Cu}^-({}^1S_o+h\nu\rightarrow{}^2S_{1/2}+e^-)$ at various wavelengths. The β values were energy independent and were very close to 2, as expected [12,34], confirming the reliability of our measurement procedure. Figure 3 shows the measured angular distribution for OH^- at 440 nm. The asymmetry parameters for the four wavelengths calculated from the measured angular distributions of photoelectrons in the OH^- photodetachment process are given in Table I. The measurements clearly indicate the energy dependence of the asymmetry parameter.

Cooper and Zare [35] describe the differential cross section for the photodetachment of an unpolarized target with linearly polarized light, under the electric dipole approximation, as

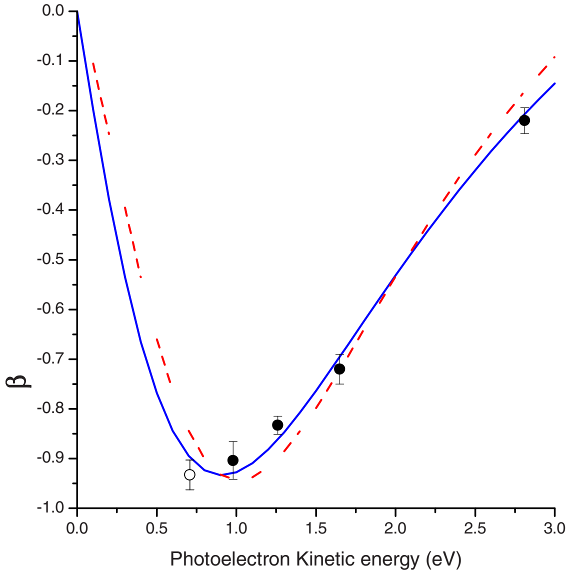

FIG. 4. (Color online) Asymmetry parameter β as a function of the photoelectron energy. The filled circles are the β parameters determined in the present work from the observed PAD for $\mathrm{OH}^-({}^1\Sigma^+)+h\nu\rightarrow\mathrm{OH}({}^2\Pi_i)+e^-$ process. The open circle represents β from a previous measurement [32]. The solid line is the least-squares fit of the observed asymmetry parameters to the dipole interaction model, represented by Eq. (6). The dashed lines represents the fit of the same to the free-electron form of the Cooper-Zare model, represented by Eq. (3).

$$\frac{d\sigma}{d\Omega} = \frac{\sigma}{4\pi}[1 + \beta/2(3\cos^2\theta - 1)] \tag{1}$$

where σ and β are the total photodetachment cross section and the asymmetry parameter, respectively.

In the Cooper-Zare central potential model for photodetachment, the ejection of a p-orbital electron should result in s and d detached electron waves, which interfere to give a characteristic photoelectron angular distribution (PAD). The asymmetry parameter in the Cooper-Zare description, using the Robinson and Geltman potential [36], is given by

$$\beta = \frac{l(l-1)R_{l-1}^2 + (l+2)(l+1)R_{l+1}^2 - 6l(l+1)R_{l-1}R_{l+1}\cos(\delta_{l+1} - \delta_{l-1})}{(2l+1)[lR_{l-1}^2 + (l+1)R_{l+1}^2]}, \tag{2}$$

where R_{l-1}, and R_{l+1} are the radial matrix elements and $\delta_{l+1} - \delta_{l-1}$ is their relative phase and $-1 \leq \beta \leq 2$. The total photodetachment cross section and the asymmetry parameter are generally energy dependent as they are functions of the transition amplitudes which depend on the energy.

To the best of our knowledge, there is no theoretical work on the spectral dependence of angular distribution for the OH^- photodetachment process. We employ the simplified form of the Cooper-Zare description as given by Hanstorp *et al.* [15]. In this model the final-state interactions are completely neglected and the radial matrix elements are assumed to vary linearly with the photoelectron kinetic energy: $R_{l\pm1} \propto k^{l\pm1}$. The photoelectron detached from OH^- originates from a π orbital, which is like the p orbital in O in the atomic picture. Under these assumptions, the asymmetry parameter is given by

$$\beta(\epsilon) = \frac{2A\epsilon(A\epsilon - 2c)}{1 + 2A^2\epsilon^2}, \tag{3}$$

where ϵ is the photoelectron kinetic energy, $A\epsilon = R_{l+1}/R_{l-1}$, and c is the cosine of the relative phase between the matrix elements.

Figure 4 shows the fit of the asymmetry parameter β determined from the measured PAD for the photodetachment from OH^- to the free-electron model described by Eq. (3). The β value at 480 nm previously determined [32] is also shown along with our PAD measurements at 400, 440, 355, and 266 nm. The values for the parameters of the least-squares fit were $A_2 = 0.54$ and $c = 0.95$.

In the presence of dipole interactions between the neutral OH and the photoelectron, the cross sections for the two allowed detachment channels are modified and hence, in principle, the spectral dependence should have the signature of the dipole interactions. O'Malley [25] modified the near-threshold cross section to include the dipole interaction between the final-state particles. In the limit of small dipole moment, the cross section for the lth partial wave is given by

$$\sigma_l = A_l k^{2\nu}, \tag{4}$$

where $\nu = [(l+1/2)^2 - \mu]^{1/2}$, μ is the dipole moment of the neutral remnant, and k is the linear momentum of the detached electron. In the limit of large dipole moment, the cross section for the lth partial wave is given by

$$\sigma_l = C_l\{\sinh^2(\pi\nu'/2) + \cos^2[(\nu' \ln k) + \delta]\}^{-1}, \tag{5}$$

where $\nu = [\mu - (l+1/2)^2]^{1/2}$. Assuming that only the radial matrix elements vary with the energy, we have $R_{l\pm1} \propto \sqrt{\sigma_{l\pm1}}$.

The asymmetry parameter, for the dipole interaction case, is then given by

$$\beta = \frac{l(l-1) + (l+2)(l+1)(\sigma_{l+1}/\sigma_{l-1}) - 6l(l+1)\sqrt{(\sigma_{l+1}/\sigma_{l-1})}\cos(\delta_{l+1} - \delta_{l-1})}{(2l+1)[l + (l+1)(\sigma_{l+1}/\sigma_{l-1})]}. \tag{6}$$

Engelking [37] and Smith *et al.* [27] discuss the origin of the dipole moment in the OH molecule. Smith *et al.* [27] in their elegant experiments studied the effect of dipole interaction on the near-threshold photodetachment cross section for OH anions. Photodetachment near the rotational thresholds would result in OH neutrals in their λ doublet states, which are states of definite parity. Such states with definite parity have no dipole moment and Smith *et al.* [27] do not observe any effect of dipole interactions on the near-threshold cross section. Engelking [37] proposed that the rotationally unresolved measurements will result in a detached electron having enough energy to mix the λ doublet states resulting in states of mixed parity, which critically determines the dipole moment of the remnant OH. In the present work, we study the dipole effects on the detached electron using rotationally unresolved experiments to understand the influence of dipole interaction on the photoelectron angular distribution. The ground state of OH is $^2\Pi_i$ and it has a nonzero component of angular momentum along the bond axis, and hence the dipole moment does not average out during the rotational motion.

Figure 4 shows the least-squares fit of the observed asymmetry parameters to Eq. (6) for $\mu_{OH}=0.65$ (atomic units) with C_2/C_0 and cos ϕ as the parameters of the fit. It is apparent from Fig. 4 that the free-electron model characterizes well the observed spectral dependence of the asymmetry parameter, and the dipole interactions do not significantly influence the spectral dependence of the asymmetry parameter. There is no theoretical calculation to determine the asymmetry parameter for the photoelectron angular distribution in the presence of dipole interactions. It should be interesting to compare the asymmetry parameter near a rotational threshold for both rotationally resolved and unresolved measurements. Figure 5 compares the fit of the free-electron model to the observed spectral dependence of β for the photodetachment from OH^- with that for the previously studied O^- [15]. The spectral dependences for both the anions are very similar. The values for the parameters in the least-squares fit for OH^- are $A_2=0.538$, $c=0.95$, and those for O^- are $A_2=0.55$ and $c=0.925$. The extra electron in OH^- seems to behave more like the p-orbital extra electron in O^-, implying no significant influence of the dipole interaction on the photoelectron angular distribution.

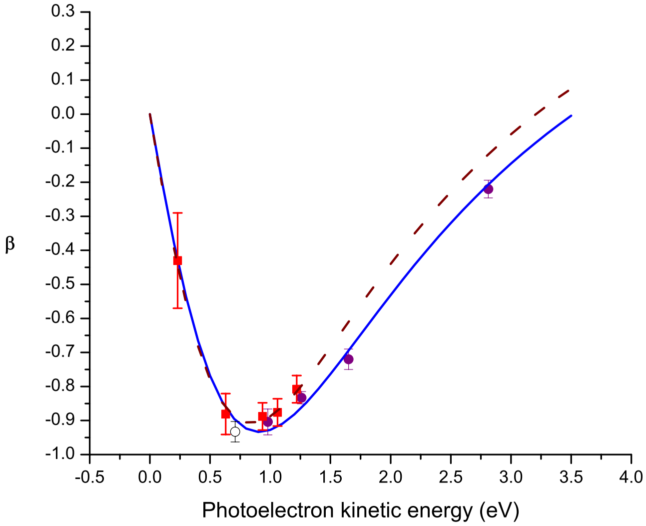

FIG. 5. (Color online) Comparison of the spectral dependences of the asymmetry parameter in the photodetachment from OH^- and O^-. The filled circles are the β parameters determined in the present work from the observed PAD for the $OH^-(^1\Sigma^+)+h\nu\rightarrow OH(^2\Pi_i)+e^-$ process, and the open circle represents β from a previous measurement [32]. Filled squares represent the asymmetry parameters for the photodetachment from O^- obtain in a previous measurement [15]. The solid and dashed lines are the least-squares fits of the observed asymmetry parameters to the free-electron model in the photodetachment from OH^- and O^-, respectively. The errors displayed are one standard deviation.

IV. SUMMARY

Angular distributions for the photodetachment from OH^- were measured at four different wavelengths using a newly constructed photoelectron spectrometer. The asymmetry parameter β shows energy dependence. The asymmetry parameters determined from the measured angular distributions at these wavelengths were fitted to a model that accounts for the dipole interaction between the final-state particles and to a free-electron form of the Cooper-Zare model. The least-squares fit of the observed spectral dependence to these two models shows absence of any significant influence of the dipole interaction between the final-state particles on the photoelectron angular distributions. It would be interesting to compare the asymmetry parameter for photodetachment near the threshold of a rotational branch for both high-resolution and rotationally unresolved measurement. Further, the spectral dependence of the asymmetry parameter in the photodetachment from OH^- is very similar to that from O^-, implying the absence of dipole or other molecular effects. We believe that the present study should motivate theoretical and experimental studies on the spectral dependence of the asymmetry parameter for molecular anions, to probe the final-state interactions.

---

[1] S. H. Massey, *Negative Ions*, 3rd ed. (Cambridge University, Cambridge, England, 1976).
[2] S. Chandrasekhar, Astrophys. J. **128**, 114 (1958).
[3] D. J. Pegg, Rep. Prog. Phys. **67**, 857 (2004).
[4] W. Demtroder, *Laser Spectroscopy* (Springer, New York, 2003).
[5] T. Andersen, Phys. Rep. **394**, 157 (2004).
[6] L. H. Andersen, T. Andersen, and P. Hvelplund, Adv. At., Mol., Opt. Phys. **38**, 155 (1997).
[7] E. Surber, R. Mabbs, and A. Sanov, J. Phys. Chem. A **107**, 8215 (2003).
[8] T. Andersen, H. K. Haugen, and H. Hotop, J. Phys. Chem. Ref. Data **28**, 1511 (1999).
[9] H. Hotop and W. C. Lineberger, J. Phys. Chem. Ref. Data **14**, 731 (1985).
[10] C. A. de Lange, J. Chem. Soc., Faraday Trans. **94**, 3409 (1998).
[11] Daniel M. Neumark, Phys. Chem. Chem. Phys. **7**, 433 (2005).
[12] S. T. Manson and A. F. Starace, Rev. Mod. Phys. **54**, 389 (1982).
[13] S. B. Whitfield, R. Wehlitz, H. R. Varma, T. Banerjee, P. C. Deshmukh, and S. T. Manson, J. Phys. B **39**, L335 (2006).
[14] G. Aravind, A. K. Gupta, M. Krishnamurthy, and E. Krishnakumar, Phys. Rev. A **75**, 042714 (2007).
[15] D. Hanstorp, C. Bengtsson, and D. J. Larson, Phys. Rev. A **40**, 670 (1989).

[16] J. S. Thompson, D. J. Pegg, R. N. Compton, and G. G. Alton, J. Phys. B **23**, L15 (1990).

[17] Y. Liu, D. J. Pegg, J. S. Thompson, J. Dellwo, and G. D. Alton, J. Phys. B **24**, L1 (1991).

[18] D. Calabrese, A. M. Covington, D. L. Carpenter, J. S. Thompson, T. J. Kvale, and R. L. Collier, J. Phys. B **30**, 4791 (1997).

[19] A. M. Covington, D. Calabrese, W. W. Williams, J. S. Thompson, and T. J. Kvale, Phys. Rev. A **56**, 4746 (1997).

[20] W. W. Williams, D. L. Carpenter, A. M. Covington, and J. S. Thompson, Phys. Rev. A **59**, 4368 (1999).

[21] V. T. Davis, J. Ashokkumar, and J. S. Thompson, Phys. Rev. A **65**, 024702 (2002).

[22] D. Calabrese, A. M. Covington, W. W. Williams, D. L. Carpenter, J. S. Thompson, and T. J. Kvale, Phys. Rev. A **71**, 042708 (2005).

[23] Richard Mabbs, Eric Srber, and Andrei Sanov, J. Chem. Phys. **122**, 054308 (2005).

[24] Eugene P. Wigner, Phys. Rev. **73**, 1002 (1948).

[25] T. F. O' Malley, Phys. Rev. **137**, A1668 (1965).

[26] Lewis M. Branscomb, Phys. Rev. **148**, 11 (1966).

[27] Jim R. Smith, Joseph B. Kim, and W. C. Lineberger, Phys. Rev. A **55**, 2036 (1997).

[28] Fabienne Goldfarb, Cyril Drag, Walid Chaibi, Sophie Kroger, Christophe Blondel, and Christian Delsart, J. Chem. Phys. **122**, 014308 (2005).

[29] Christian Delsart, Fabienne Goldfarb, and Christophe Blondel, Phys. Rev. Lett. **89**, 183002 (2002).

[30] P. A. Schultz, Roy D. Mead, P. L. Jones, and W. C. Lineberger, J. Chem. Phys. **77**, 1153 (1982).

[31] H. Hotop, T. A. Patterson, and W. C. Lineberger, J. Chem. Phys. **60**, 1806 (1974).

[32] R. J. Celotta, R. A. Bennett, and J. L. Hall, J. Chem. Phys. **60**, 1740 (1974).

[33] A. K. Gupta and P. Ayyub, Eur. Phys. J. D **17**, 221 (2001).

[34] H. Hotop, R. A. Bennett, and W. C. Lineberger, J. Chem. Phys. **58**, 2373 (1973).

[35] J. Cooper and R. N. Zare, J. Chem. Phys. **48**, 942 (1968).

[36] E. J. Robinson and S. Geltman, Phys. Rev. **153**, 4 (1967).

[37] P. C. Engelking, Phys. Rev. A **26**, 740 (1982).